Calibration of (57)Fe Mössbauer constants by first principles

Calibration of ^{57}Fe Mössbauer constants by first principles

Silvia Casassa * and Anna Maria Ferrari

Dipartimento di Chimica and Centre of Excellence NIS (Nanostructured Interfaces and Surfaces), Università degli Studi di Torino, via P. Giuria 5, I-10125 Torino, Italy. E-mail: silvia.casassa@unito.it

Abstract

Electron density and eigenvalues of the 3 × 3 matrix of the electric field gradients at the ^{57}Fe nuclei positions have been evaluated with the periodic *ab initio* CRYSTAL code for a wide range of crystalline compounds, adopting different computational approaches (Hartree–Fock, gradient corrected and hybrids functionals). The robust calibration procedure, involving experimental isomer shifts and quadrupolar splittings, yields reliable Mössbauer parameters, *i.e.* the isomer shift constant (α) and the nuclear quadrupolar moment (Q). Dependence of the results on the Hamiltonian is explored and well suited localized basis sets for periodic calculations are provided.

1 Introduction

When a γ ray, emitted from a nuclear source, interacts with an identical nucleus in a different environment, resulting in the corresponding absorption between the nuclear spin states, three phenomena are responsible for the observed frequency shift and splitting: (i) the isotropic effect (ii) the

quadrupolar interaction and (iii) the magnetic splitting. Experimentally, the shifts and splittings are measured by means of Mössbauer spectroscopy.

The first two effects originate from the interaction between the nuclear charge distribution and the electric field due to the surrounding electrons. Their determination can provide important information on the chemical environment surrounding the absorbing nucleus. ^{57}Fe, with its ability to form compounds that exhibit a wide range of bonding situations, ranging from pure ionic to pure covalent, is the most studied isotope by the Mössbauer technique.

First-principle approaches, especially on cluster models, have demonstrated that a rather accurate calibration of α[1–9] and Q[4,10–12] can be achieved. The fitting procedure for iron has shown a remarkable robustness[5,6] in the sense that both parameters are well determined provided a broad sample of oxidation states, electronic spin states, and compounds with different coordination number are included.

There are still a few issues that remain under consideration: (i) the electron density at the nucleus strongly depends on the adopted functional and is, thus, not universal. One issue is to what extent the difference in this property between different environments, which is ultimately what matters, depends upon the computational method. (ii) Another issue is the choice of basis set, particularly with regard to describing the small, but important, aspherical distortions of the 3p shell. In this connection a basis set with enhanced flexibility in the core region has been proposed.[2] (iii) In addition, the effect of electron correlation on the key parameters has yet to be fully elucidated. (iv) Finally, the uncertainty in the experimental value of the quadrupole moment of ^{57}Fe makes the theoretical analysis more complicated, although still feasible, and interesting.

In the present research we use the CRYSTAL14 program[13,14] to estimate α and Q for a variety of crystalline inorganic ^{57}Fe compounds, exploiting the additional information provided by a generalization of the Fermi contact calculation performed by the authors. A large range of crystalline materials have been included in this calibration set. For the first time in periodic DFT calculations, in addition to generalized gradient approximate functionals (GGA) hybrid schemes are also tested. In the latter case the percentage of exact Hartree–Fock (HF) exchange is varied from 20% up to 60% and pure HF calculations are done as well. Relativistic effects are neglected, which leads to unrealistic absolute values of $\rho(\mathbf{r})$, although changes in electron density among a series of compounds are accurately predicted. As expected, EFGs were found to be a much more sensitive property[15–17] and a fairly good linear correlation was obtained only at the GGA level.

This paper is organized as follows. First, the main equations of the linear response approach[18,19] are presented; then, computational parameters are specified followed by the results and their

discussion. Finally, general conclusions are drawn and tentative solutions for some of the issues previously raised are proposed.

2 Theory

The Mössbauer effect consists of the recoilless, resonant emission and absorption of a γ ray in a nuclear spin transition. In the case of the most common Mössbauer nucleus, ^{57}Fe, the energy difference between the two spin states, corresponding to $I = 1/2 \rightarrow I = 3/2$, occurs at 14.4 keV.

The overall electrostatic energy, E, due to the interaction between the nuclear charge density and the electronic Coulomb potential $V(\mathbf{r})$ may be factorized into the isotropic (*i.e.* spherical) and anisotropic parts of the electronic charge distribution.

The isotropic contribution, after truncating at the second order in the Taylor series expansion of the Coulomb potential, can be calculated by exploiting Poisson's equation ($\nabla^2 V(\mathbf{r}) = -\rho(\mathbf{r})/\varepsilon_0$):

$$E_{\mathrm{iso}} = \frac{2\pi Ze^2}{5\varepsilon_0}\mathbf{r}_n^{\,2}\rho(\mathbf{r}_n) \tag{1}$$

Here $\mathbf{r}_n$ is the nuclear radius and ε_0 is the dielectric constant, with Ze and e equal, respectively, to the magnitude of the nuclear and electronic charges. Because the average value of $\mathbf{r}_n$ depends on the spin state, the energy difference between the states I and I' can be written as:[18,20]

$$\Delta E_{\mathrm{iso}} = \frac{2\pi Ze^2}{5\varepsilon_0}\left[\mathbf{r}_n'^{\,2} - \mathbf{r}_n^{\,2}\right]\rho(\mathbf{r}_n) \tag{2}$$

under the assumption that the electron density is unaffected by the nuclear transition,[2] *i.e.* $\rho(\mathbf{r}_n) \equiv \rho(\mathbf{r}_n')$. The effective radius of the iron ground state, which is ≈4.9 fm,[4,21] is much larger than that of its excited state[20] and then eqn (2) can be recast in a different form by defining $\delta\mathbf{r}_n = \mathbf{r}_n' - \mathbf{r}_n$ and $\mathbf{r}_n' + \mathbf{r}_n \approx 2\mathbf{r}_n$:

$$\Delta E_{\mathrm{iso}} = \frac{4\pi Ze^2}{5\varepsilon_0}\mathbf{r}_n^{\,2}\left(\frac{\delta\mathbf{r}_n}{\mathbf{r}_n}\right)\rho(\mathbf{r}_n) \tag{3}$$

The approximation made here is justified by the general observation that $\delta\mathbf{r}_n/\mathbf{r}_n$ is usually on the order of 0.001[18] (1.8×10^{-3} for iron[20]).

What is observed experimentally is the shift, δ, of the Doppler velocity necessary to achieve the resonant absorption between the source, S, and the probe nucleus, A, usually expressed in mm s^{-1} and referred to as the isomer shift:

$$\delta = \frac{c}{E_\gamma}\left[\Delta E_{\mathrm{iso}}^{\mathrm{A}} - \Delta E_{\mathrm{iso}}^{\mathrm{S}}\right] \tag{4}$$

In eqn (4) c is the speed of light and E_γ is the energy of the incident γ photon. If we assume that the fractional variation of the nuclear charge radius is the same for both S and A, then:

$$\delta = \frac{c}{E_\gamma}\frac{4\pi Z e^2}{5\varepsilon_0}\mathbf{r}_n^{\,2}\left(\frac{\delta \mathbf{r}_n}{\mathbf{r}_n}\right)\left[\rho^{\mathrm{A}}(\mathbf{r}_n) - \rho^{\mathrm{S}}(\mathbf{r}_n)\right] \tag{5}$$

This expression shows that the isomer shift is directly proportional to the difference in electron density at the nucleus depending upon the chemical environment.

It is worth noting that relativistic corrections have an important effect on δ. In order to obtain a realistic estimate of the electron density at the nucleus, a dimensionless multiplicative correction factor ($S(Z)$), independent of spin state, has been proposed. For iron it is estimated to be given by $\rho(\mathbf{r}_n)^{\mathrm{rel}} = 1.32\rho(\mathbf{r}_n)$.[18] Since all the terms in eqn (5) are constant for a given isotope except for the electron density, it is sufficient to consider the following simplified equation:

$$\delta = \alpha[\rho^{\mathrm{A}}(\mathbf{r}) - b] \tag{6}$$

where α and b are determined by a calibration procedure.[18–20,22] In this procedure the calculated electron density at a given nucleus, considered as a point charge of zero radius is plotted *versus* the experimentally measured δ, for a set of compounds containing that nucleus.[1,2,4,23]

The anisotropic contribution is due to the interaction between the electric field gradients (EFG), *i.e.* the second derivatives of the electrostatic potential, $V_{xy} = \frac{\partial^2 V}{\partial x \partial y}$, and the nuclear quadrupole moment, Q, which represents the deviation of the nuclear charge from the ideal spherical shape:

$$E_{\mathrm{aniso}} = e^2 \sum_{i,j=x,y,z} V_{ij}Q_{ij} = VQ \tag{7}$$

Diagonalization of V yields the three components in the principal axis system and, given the convention $|V_{XX}| < |V_{YY}| < |V_{ZZ}|$, an asymmetry parameter, η, can be defined as:

$$\eta = \frac{V_{YY} - V_{XX}}{V_{ZZ}} \tag{8}$$

The anisotropic term is responsible for splitting the $I = 3/2$ excited nuclear spin state into two doubly degenerate components characterized by the magnetic quantum numbers $M_{I=3/2} = \pm 1/2, \pm 3/2$, which

leads to the quadrupolar splitting:

$$\Delta E_Q = \frac{1}{2} eQV_{ZZ}\left(1+\frac{\eta^2}{3}\right)^{1/2} \quad (9)$$

Similar to the case of α, the calculation of the nuclear quadrupole moment is obtained by plotting the experimental ΔE_Q as a function of the EFG parameters V_{ZZ} and η.[24,25]

3 Computational details

Electron contact densities and the components of the EFG tensor at the ^{57}Fe nucleus were calculated with the latest version of the *ab initio* CRYSTAL suite of programs.[13,14] CRYSTAL solves the Schrödinger equation for periodic systems in a basis set consisting of contracted Gaussian-type atomic orbitals. With regard to the Hamiltonian, several different types of approximation were tested including (i) three pure GGA functionals: Perdew–Burke–Ernzerhof[26] (PBE) Perdew–Wang[27,28] (PWGGA) and one of the Minnesota set proposed by Truhlar and co-workers[29] (M06L); (ii) four hybrid functionals: B3LYP,[30,31] PBE0,[32] and the new global hybrids meta-GGA M06[33] and M062X,[33] containing 20%, 25%, 27% and 50% of Hartree–Fock (HF) exact exchange, respectively; and (iii) the HF method.

In the numerical integration of the DFT exchange–correlation term an extra-large pruned grid, consisting of 99 radial and 1454 angular points, selected according to a Lebedev scheme, was adopted.[14] The level of accuracy in evaluating the Coulomb and exchange integrals is controlled by five parameters, T^i_1–T^i_5, that were set to 8 8 8 15 and 30 in present calculations.[14] Reciprocal space is sampled regularly, according to a sub-lattice with shrinking factor set equal to 12, corresponding to a number of independent *k*-points in the irreducible part of the first Brillouin zone (1BZ) ranging from a minimum of 72, in the case of α-Fe, to 189 in FeF_3, depending on the reciprocal lattice symmetry. It should be noted that, when 72 points are included in the 1BZ, the total number of *k*-points for, say, a cubic lattice is 868.

Iron was described using the Wachters basis set,[34] from which the most diffuse p and d functions were removed to avoid problems of linear dependence during the self-consistent field procedure. The resulting [6211111-33121-311]/(7s/5p/3d) basis provides a satisfactory description of the total electron density at the Fe nucleus: our PBE result is 11 616 a.u.$^{-3}$, in good agreement with the non-relativistic DFT value of 11 607 a.u.$^{-3}$ by Wdowik and Ruebenbauer. Some test calculations were also performed with the basis set CP(PPP) developed by Neese for cluster calculations.[2] In this case, the most diffuse s and p functions were removed, leading to a [1111111111111111-331111-311-1]/(16s/6p/3d/1f) basis.

The electron density at the iron nucleus calculated at the CP(PPP)/HF level is 11 822, which may be compared with 11 873 obtained by Walker *et al.*[20] and 11 860 due to Moruzzi and Janak.[35]

In the following the Wachters basis set for iron is always utilized unless otherwise specified. The triple-zeta valence basis set with Polarization functions (TZVP) optimized for solid state applications,[36,37] were used for all the other atoms.

Mössbauer constants have been obtained adopting the linear response approach[2,11,22,23] on the non-relativistic point-like nucleus of ^{57}Fe, for crystals in their experimental geometry.

The TOPOND program, developed by C. Gatti[38] and recently embedded in CRYSTAL14,[39] has been used in the determination of ^{57}Fe topological properties (charge, spin, Laplacian) according to a Bader analysis of the electron density in molecules[40] and crystals.[41]

4 Results

4.1 The calibration set

The confidence with which α and Q can be generally used in the prediction of unknown isomer and quadrupolar shifts, strongly depends on the variety of systems included in the reference set. Both, δ and ΔE_Q are sensitive reporters of the spin and valence state of a nucleus, as well as the degree of covalency/ionicity of its bonding network, we have considered iron compounds with a variety of oxidation states and coordination. The high spin Fe^{2+} state is represented by four anti-ferromagnetic (AF) crystals: FeF_2,[42] $FeCl_2$,[43] $FeBr_2$,[44] and FeI_2.[45] All of them have axially symmetric EFG tensors, namely zero value of η, except FeF2.[46] The stoichiometric AF insulators FeF_3[47] and $FeCl_3$[48] have been included to model the high spin Fe^{3+} configuration. Then, two oxides were considered, Fe_2O_3[49] and FeO,[50] and the non-magnetic TiFe[51] and AlFe[52] phases were selected as representative of metal states. The reference system, experimentally an iron foil, labeled with S in previous equations, was simulated modeling the α-Fe, which is the ordered ferro-magnetic low spin body-centered phase of iron. Structural data for each compound in its experimental geometry and information on the iron net charge and spin density, as evaluated at the PBE0 level, are collected in Table 1. Data for the other Hamiltonians are reported in Table S1 of the ESI.†

Table 1 Experimental crystallographic data of the systems included in the calibration set. Lattice constants and distances are given in Å. X stands for F, Cl, Br, I, O, Al, Ti. The Bader net charge, Q_{net}, and spin density, μ, of ^{57}Fe, in a.u., was evaluated at the PBE0 level

System		*a*	*c*	*d*(Fe–X)	Q_{net}	μ
FeF_2[42]	($P4_2/mnm$)	4.697	3.308	2.00	1.63	3.76

System		a	c	d(Fe–X)	Q_{net}	μ
$FeCl_2$ [43]	($P\bar{3}m1$)	3.585	5.735	2.49	1.34	3.71
$FeBr_2$ [44]	($P\bar{3}m1$)	3.772	6.223	2.68	1.22	3.73
FeI_2 [45]	($P\bar{3}m1$)	4.050	6.750	2.84	0.96	3.73
FeO [50]	($Fm3m$)	4.363	—	2.18	1.44	3.72
FeF_3 [47]	($R\bar{3}c$)	5.362	13.329	1.92	2.23	4.42
$FeCl_3$ [48]	($R\bar{3}c$)	6.065	17.440	2.38	1.65	4.17
Fe_2O_3 [49]	($R\bar{3}c$)	5.038	13.772	1.94	1.96	4.30
AlFe [52]	($Pm\bar{3}m$)	2.910	—	2.52	−1.45	0.0
Fe	($Im\bar{3}m$)	2.831	—	2.45	0.01	2.78
TiFe [51]	($Pm\bar{3}m$)	2.976	—	2.58	−1.04	0.0

4.2 Mössbauer parameters

Calculated values of isomer shift constants are collected in Table 2. For sake of clarity, all the computed data for each Hamiltonian, together with the experimental values used in the regression procedure, are reported in Table S2 of the ESI. †

Table 2 Linear fit data for ^{57}Fe using eqn (6). Correlation coefficient, R, and standard deviation, σ, measure the quality of the linear fit. Electron density on ^{57}Fe in α-Fe phase is the reference. Computed α values from the literature, which are referred to in the text, are added in parentheses. Fitting data can be found in Table S2 of the ESI

Func. (% HF_{exch})	α (mm s^{-1})	$\rho_e(r)$ (bohr^{-3})	R	σ (mm s^{-1})
PBE (0)	−0.420 (−0.291 [4])	11 616	−0.97	0.14
PWGGA (0)	−0.420	11 616	−0.97	0.14
M06L (0)	−0.411	11 629	−0.98	0.11
B3LYP (20)	−0.393 (−0.366 [3])	11 614	−0.98	0.11
PBE0 (25)	−0.364	11 618	−0.98	0.10
M06 (27)	−0.455	11 628	−0.98	0.10
M062X (54)	−0.327	11 595	−0.98	0.15
HF (100)	−0.254 (−0.265 [6])	11 624	−0.97	0.13
Exp.	−0.31 ± 0.04 [55]			

The importance of including relativistic and electron correlation effects for a correct estimate of the absolute value of the Fermi contact term has already been discussed and demonstrated elsewhere.[5,6] However, as already stated, because both isomer and quadrupolar shifts are relative quantities that depend only on the contact density difference it can be assumed, without lost of generality, that they are independent of electron correlation and relativistic effects.[9] In fact, this procedure shows a fairly good linear relation between the shifts and the difference in contact density (correlation coefficients $R = 0.97 \pm 0.1$) and the results are also in the range of experimental measurements. Our data confirm the sensitive dependence of α on the adopted functional; its value goes from −0.420 (PBE) to −0.254 (HF) with a monotonic decrease as the percentage of HF exchange in the functional increases. A comparison between the three approaches – namely pure GGA, hybrid and HF – is shown in Fig. 1 where the experimental isomer shift, δ, is plotted *versus* the difference in electron density on ^{57}Fe. This behavior is not unexpected and has already been observed by Neese[5] who was the first to propose that a separate correlation should be established for each combination of functional and basis set.

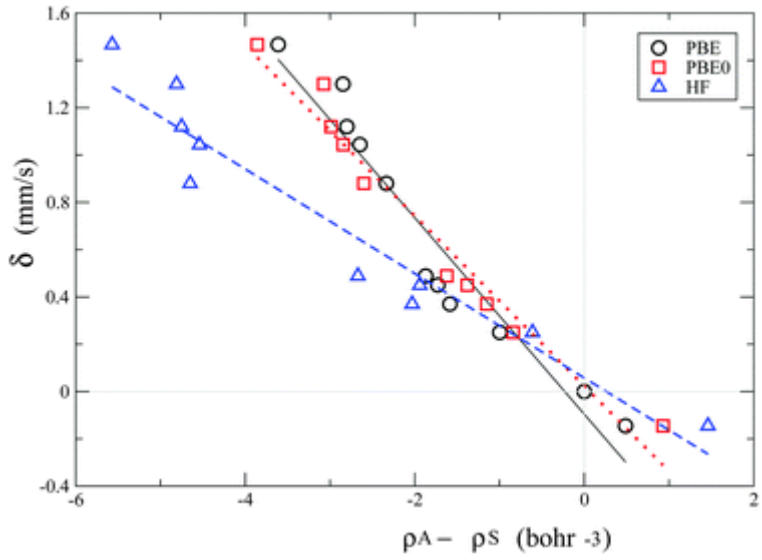

Fig. 1 Experimental isomer shift *versus* difference in electron density at the ^{57}Fe nucleus for all the compounds in the calibration set.

A comparison of our value of α with the PBE value of Wdowik and Ruebenbauer,[4] reported in Table 2 shows an unpleasant discrepancy that can be ascribed to their extension of the simplified point-like model for the contact interaction. Our results are in better agreement with the B3LYP cluster calculations performed by Neese and coworkers,[3,53] and the HF data of Filatov *et al.*[6,54]

A possible explanation for the lowering of the regression coefficient in the HF case can be found in the different description of electron density and related properties. At the HF level bonds are slightly

more ionic and charge tends to flow to the more electronegative atoms. As a consequence, the difference in electron density with respect to the reference metallic system is more pronounced and for a given set of experimental data, the slope of the linear fit is reduced. Topological data can be used to support this interpretation. On the basis of the value of the potential *vs.* kinetic energy ration at the bond critical point[38] the Fe–X_2 interactions, with X = F, Cl, Br, are classified as ionic only at the HF level. The other Hamiltonians describe the bonding as neither covalent nor ionic.[41]

The same set of compounds has been used for the estimate of Q, apart from metals and FeO whose EFG components are zero due to symmetry reasons. As regards FeO, the observed quadrupolar splitting (0.3 mm s^{-1}) was an unexpected result that has been ascribed to a local distortion from cubic symmetry at the Fe site due to the significant presence of cation vacancies in the sample.[25]

As in the case of α, the calculated data and experimental quadrupolar splittings are reported in the ESI,† in Table S3. Results of the regression procedure are collected in Table 3 and, although the accuracy of the fitting is lower ($R = 0.86 \pm 0.1$) PBE, PWGGA and M06L provide a value of $Q = 0.12$ barn, which is in satisfactory agreement with the data of Blaha *et al.*[11] and Wdowik and Ruebenbauer.[4] In addition, the asymmetry parameter, η, for FeF_2, is accurately reproduced by the GGA methods.

Table 3 Linear fit results for the asymmetry parameter, η, and the nuclear quadrupole moment, Q, at ^{57}Fe in FeF_2 obtained using eqn (6). Data used in the fitting procedure are collected in Table S3 of the ESI

Func.	Q (barn)	η (e a_0^{-3})	R
PBE	0.12	0.2	0.86
PWGGA	0.12	0.2	0.85
M06L	0.13	0.3	0.89
Others	0.16,[11] 0.17[4]	0.3	
Exp.		0.4[46]	

As already pointed out by others[3,17] hybrid exchange–correlation functionals completely fail for the prediction of quadrupolar splitting. The inaccuracies of hybrid methods ($R \approx 0.4$ for PBE0 and B3LYP) can probably be ascribed to the difficulty that HF has in reproducing the correct shape of the electronic charge distribution at the nucleus. In order to support this hypothesis we have performed an analysis of the Laplacian of the charge density, $L(\mathbf{r}) = \nabla^2\rho(\mathbf{r})$, on FeF_2 and $FeCl_2$. Iron fluoride is perfectly described at any level whereas the EFGs of $FeCl_2$ are wrongly predicted when HF or hybrid approaches are adopted. $L(\mathbf{r})$ exhibits a shell structure with negative and positive values in regions of charge concentration or depletion and, in contrast to charge density, it can often reveal non-sphericality of the

electronic charge distribution close to the nucleus. In Fig. 2, we have reported differences between $L(\mathbf{r})$ as calculated by TOPOND with the three methods. Some comments can be made: (i) it is possible to infer that the overall basin distribution of $L(\mathbf{r})$ influences the value of EFGs at the nucleus; (ii) HF exchange, even in small percentage, is dominant in defining the symmetry of the distribution and (iii) in FeF_2, where HF does not fail, the cylindrical symmetry is retained while in $FeCl_2$ a certain degree of anisotropy is lost at the hybrid/HF level.

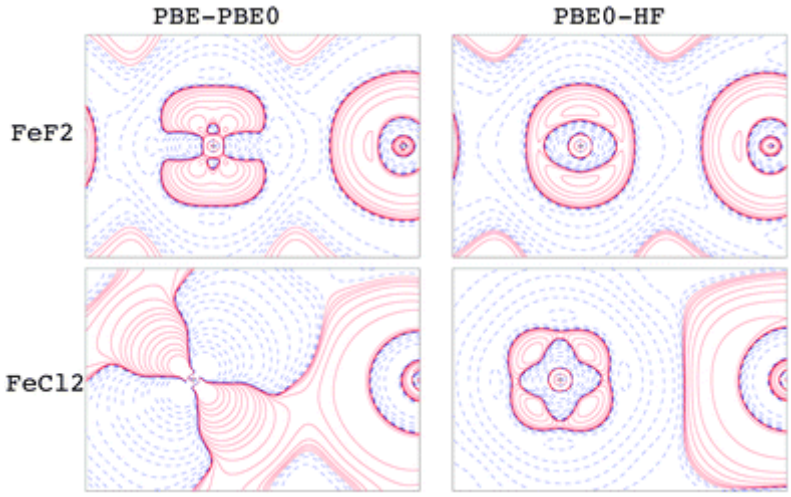

Fig. 2 Difference of the Laplacian of the electron density, $\nabla^2\rho(\mathbf{r}_n)$ in the plane containing Fe (left side of each panel) and Cl (right side) atoms, in FeF_2 (top) and $FeCl_2$ (bottom) respectively. PBE0 values are subtracted from PBE results (left column) and HF values are subtracted from PBE0 results (right column). A logarithmic scale is adopted between −8 and 8 a.u. Continuous red lines and dotted blue lines indicate positive and negative contours, respectively.

Finally, to verify possible effects due to the basis set in the calculation of EFGs, the CP(PPP) basis of Neese[2] has been used with PBE. Our results, detailed in Table S2 of the ESI,† reproduce the previous findings, *i.e.* $Q = 0.13$ barn and $R = 0.86$. This proves, once again, that EFGs are strictly related to how the different Hamiltonians describe $\rho(\mathbf{r})$ and its derivatives at the nucleus.

5 Conclusions

In this work, Mössbauer parameters for a wide range of inorganic crystalline compounds containing the ^{57}Fe isotope have been studied at the *ab initio* periodic level, with a basis set of localized Gaussian-type atomic orbitals. HF, pure GGA and hybrid Hamiltonians were utilized.

The isomer shift constant, α, was inferred with high accuracy on the basis of a robust calibration procedure.[2,18,23] It has been shown that the best agreement with the experimental value is achieved

when 20–25% of HF exact-exchange is included in the functionals (B3LYP, PBE0).

A good estimate of the nuclear quadrupolar moment was achieved only at the GGA level, thereby endorsing the results of others research groups.[4,11]

As already discussed by other authors in the case of finite systems,[5] the use of large set of s functions for the description of the iron core density does not significantly improve the results of non-relativistic calculations. Reliable values of Mössbauer parameters can be achieved by employing a standard basis set of triple zeta quality.

Our parameters can be confidently used to investigate compounds containing ^{57}Fe in different environments provided that the same computational framework is adopted.

References

1. O. Eriksson and A. Svane , *J. Phys.: Condens. Matter*, 1989, **1** , 1589.
2. F. Neese *Inorg. Chim. Acta*, 2002, **337** , 181 —192.
3. S. Sinnecker , L. D. Slep , E. Bill and F. Neese , *Inorg. Chem.*, 2005, **44** , 2245 —2254.
4. U. D. Wdowik and K. Ruebenbauer , *Phys. Rev. B: Condens. Matter Mater. Phys.*, 2007, **76** , 155118.
5. M. Römelt , S. Ye and F. Neese , *Inorg. Chem.*, 2009, **48** , 784 —785.
6. R. Kurian and M. Filatov , *Phys. Chem. Chem. Phys.*, 2010, **12** , 2758.
7. A. M. M. Navarro , C. Torres and L. Errico , *Hyperfine Interact.*, 2011, **202** , 117 —121.
8. J. Gubler , A. Finkelmann and M. Reiher , *Inorg. Chem.*, 2013, **52** , 14205.
9. E. Hedegård , S. Knecht , U. Ryde , J. Kongsted and T. Saue , *Phys. Chem. Chem. Phys.*, 2014, **16** , 4843.
10. K. Duff , K. Mishra and T. Das , *Phys. Rev. Lett.*, 1981, **46** , 1611.
11. P. Dufek , P. Blaha and K. Schwarz , *Phys. Rev. Lett.*, 1995, **75** , 3545.
12. G. Martinez-Pinedo , P. Schwerdtfeger , E. Caurier , K. Langanke , W. Nazarewicz and T. Söhnel , *Phys. Rev. Lett.*, 2001, **87** , 062701.
13. R. Dovesi , R. Orlando , A. Erba , C. M. Zicovich-Wilson , B. Civalleri , S. Casassa , L. Maschio , M. Ferrabone , M. D. la Pierre , P. D'Arco , Y. Noël , M. Causà , M. Rerat and B. Kirtman , *Int. J. Quantum Chem.*, 2014, 1287 —1317.
14. R.Dovesi, V. R.Saunders, C.Roetti, R.Orlando, C. M.Zicovich-Wilson, F.Pascale, B.Civalleri, K.Doll, N. M.Harrison, I. J.Bush, P.D'Arco, M.Llunell, M.Causà and Y.Noel, CRYSTAL 2014 User's Manual, 2014.
15. R. Axtmann , Y. Hazony and J. Hurley. Jr. , *Chem. Phys. Lett.*, 1968, **2** , 673.
16. F. Hagelberg , T. Das and K. Mishra , *Phys. Rev. B: Condens. Matter Mater. Phys.*, 2001, **65** , 014425.
17. V. Nemykin and R. G. Hadt , *Inorg. Chem.*, 2006, **45** , 8297 —8307.
18. D. Shirley *Rev. Mod. Phys.*, 1964, **36** , 339.
19. K. Duff *Phys. Rev. B: Condens. Matter Mater. Phys.*, 1974, **9** , 66.
20. L. Walker , G. Wertheim and V. Jaccarino , *Phys. Rev. Lett.*, 1961, **6** , 98.
21. L. R. B. Elton *Nuclear Sizes* , Oxford University Press, Oxford, UK, 1961.

22. G. Wertheim *Phys. Rev.*, 1961, **121** , 63.
23. M. Filatov *J. Chem. Phys.*, 2007, **127** , 084101.
24. R. Ingalls *Phys. Rev.*, 1964, **133** , A787.
25. G. Shirane , D. E. Cox and S. Ruby , *Phys. Rev.*, 1962, **4** , 1158.
26. J. Perdew , K. Burke and M. Ernzerhof , *Phys. Rev. Lett.*, 1996, **77** , 3865.
27. J. P. Perdew and Y. Wang , *Phys. Rev. B: Condens. Matter Mater. Phys.*, 1986, **33** , 8800.
28. J. P. Perdew and Y. Wang , *Phys. Rev. B: Condens. Matter Mater. Phys.*, 1992, **45** , 13244.
29. Y. Zhao and D. G. Truhlar , *J. Chem. Phys.*, 2006, **125** , 194101.
30. A. Becke *J. Chem. Phys.*, 1993, **98** , 5648.
31. C. Lee , W. Yang and R. G. Parr , *Phys. Rev. B: Condens. Matter Mater. Phys.*, 1998, **37** , 785.
32. C. Adamo and V. Barone , *J. Chem. Phys.*, 1999, **110** , 6158.
33. Y. Zhao and D. G. Truhlar , *Theor. Chem. Acc.*, 2008, **120** , 215.
34. A. Wachters *J. Chem. Phys.*, 1970, **52** , 1033.
35. A. R. Williams , V. L. Moruzzi and J. F. Janak , *Calculated Electronic properties of Metals* , Pergamon Press, 1978.
36. M. F. Peintinger , D. V. Oliveira and T. Bredow , *J. Comput. Chem.*, 2012, **34** , 451 —459.
37. http://www.crystal.unito.it/basis-sets.php, 2014
38. C. Gatti , V. R. Saunders and C. Roetti , *J. Chem. Phys.*, 1994, **101** , 10686.
39. C.Gatti and S.Casassa, TOPOND-2013 User's manual, CNR-CSRSRC, Milano, 2013.
40. R. F. W. Bader *Atoms in Molecules – A Quantum Theory* , Oxford University Press, Oxford, UK, 1990.
41. C. Gatti *Z. Kristallogr.*, 2005, **220** , 399.
42. W. Jauch , A. Palmer and J. Schultz , *Acta Crystallogr.*, 1993, **B49** , 984 —987.
43. R. de Kouchkovsky and J. Nasser , *J. Phys.*, 1986, **47** , 1741 —1749.
44. M. Wilkinson , J. Cable , E. Wollan and W. Koehler , *Phys. Rev.*, 1959, **113** , 497.
45. J. Gelard , A. Fert , P. Meriel and Y. Allain , *Solid State Commun.*, 1974, **14** , 187.
46. G. Wertheim and D. Buchanan , *Phys. Rev.*, 1967, **161** , 478.
47. F. Morral *J. Met.*, 1958, **10** , 662 .
48. S. Hashimoto , K. Forster and S. C. Moss , *J. Appl. Crystallogr.*, 1988, **22** , 173 —180.
49. H. Fjellvag , B. C. Hauback , T. Vogt and S. Stolen , *Am. Mineral.*, 1988, **51** , 123 —129 .
50. M. Radler , J. Cohen and J. Faber , *J. Phys. Chem. Solids*, 1990, **51** , 217 —228 .

51. D. Papaconstantopoulos *Phys. Rev. B: Condens. Matter Mater. Phys.*, 1975, **11** , 4801 .
52. J. Koch , N. Stefanou and C. Koenig , *Phys. Rev. B: Condens. Matter Mater. Phys.*, 1986, **33** , 5319.
53. F. Neese *Wiley Interdiscip. Rev.: Comput. Mol. Sci.*, 2012, **2** , 73 —78.
54. E.Kraka, J.Gräfenstein, M.Filatov, V.Polo, A.Wu, Y.He, L.Olsson, Z.Konkoli, Z.He, J.Gauss, F.Reichel and D.Cremer, Computer code COLOGNE 2005, 2005.
55. J. Ladrière , A. Meykens , R. Coussement , M. Cogneau , M. Boge , P. Auric , R. Bouchez , A. Benabed and J. Godard , *J. Phys. Colloid Chem.*, 1979, **40** , 20.